Scientific and Social Research, 2026, Volume 8, Issue 2
https://ojs.bbwpublisher.com/index.php/SSR
Online ISSN: 2981-9946
Print ISSN: 2661-4332

SRB-Induced Corrosion Behavior and Mechanisms of MIC-Resistant Pipeline Steel under High-Pressure Conditions

Shuting Zhang[1], **Maocheng Yan**[2]*, **Bowen Gao**[2]

[1]Shenyang Ligong University, Shenyang 110159, Liaoning, China
[2]Institute of Metal Research, Chinese Academy of Sciences, Shenyang 110016, Liaoning, China

**Author to whom correspondence should be addressed.*

Abstract: To investigate the microbiologically influenced corrosion behavior of pipeline steel under the combined action of high pressure and high chloride ion (Cl-) concentration, this study conducted high-pressure immersion experiments containing sulfate-reducing bacteria (SRB) on hot-rolled antibacterial steel, quenched and tempered antibacterial steel, and conventional steel. Corrosion rates, corrosion products, and corrosion morphology were systematically analyzed and compared. The results indicate that high pressure and high Cl- concentration are the primary environmental factors promoting concurrent uniform corrosion and localized pitting. All three steels exhibited the highest corrosion severity under the most severe conditions. The quenched and tempered antibacterial steel consistently maintained the lowest average corrosion rate and controlled pitting depth across various conditions. The corrosion behavior of the hot-rolled antibacterial steel was influenced by the integrity of its product film and biofilm, while the conventional steel was more susceptible to severe localized corrosion under high pressure. Microscopic analysis revealed that the characteristics of corrosion products and biofilm structure jointly determine the differences in corrosion resistance.

Keywords: Microbiologically influenced corrosion; Sulfate-reducing bacteria; Pipeline steel

Online publication: March 18, 2026

1. Introduction

Corrosion is a pervasive phenomenon across various engineering fields. It not only degrades material performance and shortens the service life of equipment or structures but can also lead to serious safety incidents [1–4]. In oilfield production, pipeline steel corrosion has long been a widespread problem. Research indicates that microbiologically influenced corrosion (MIC) is a major cause of pipeline material degradation and failure, resulting in significant economic losses, with numerous related cases reported both domestically and internationally [5–6]. Among various microorganisms, sulfate-reducing bacteria (SRB) are typical bacteria that induce or accelerate material corrosion, causing the most extensive and impactful corrosion damage [7]. SRB accelerates the corrosion process of metallic materials through their metabolic activities. These microorganisms can utilize dissolved oxygen, sulfides, etc., present in pipelines as energy sources, producing corrosive substances. Furthermore, certain SRB can directly influence iron through electron transfer, a mechanism known as electrochemical microbiologically influenced corrosion (EMIC) [8]. To address MIC, researchers have proposed various protective measures. Among them, copper-bearing pipeline steel is an effective solution. By adding an appropriate amount of copper to the pipeline steel, bacteria can be killed, and the formation of bacterial biofilms can be inhibited, thereby providing resistance to MIC [9]. Most existing studies have been conducted under atmospheric pressure. However, in the actual high-pressure environments of deep oil and gas extraction, elevated CO_2 partial pressure leads to a significant decrease in solution pH, exacerbating uniform metal corrosion. Simultaneously, high pressure may alter the physiological activity and metabolic pathways of SRB and affect the stability and structure of corrosion product films and biofilms [10]. This study investigates the corrosion behavior of MIC-resistant pipeline steels under high-pressure SRB-containing environments, focusing on the coupled effects of CO_2 partial pressure, Cl^- concentration, and microbial activity.

2. Experimental section: Preparation of experimental materials

The materials used in this study included L245 antibacterial steel in the hot-rolled and tempered condition, L360 antibacterial steel in the quenched and tempered condition, and quenched and tempered non-antibacterial steel for comparison. The SRB strain was isolated from deposits on the inner wall of a gathering pipeline in the Daqing Oilfield and enriched using API RP-38 medium [11]. The enriched culture was stored at 4 °C prior to use.

The simulated corrosion solution was prepared based on API RP-38 medium, with chloride ion concentrations adjusted to 15,000 mg/L and 50,000 mg/L. The medium consisted of NaCl (10.0 g/L), $MgSO_4 \cdot 7H_2O$ (0.2 g/L), sodium lactate (4.0 g/L), K_2HPO_4 (0.5 g/L), and ascorbic acid (0.1 g/L). The pH was adjusted to 7.0–7.2 using 1 mol/L NaOH. To ensure anaerobic conditions, the medium was purged with high-purity N_2 for 2 h and sterilized at 121 °C for 30 min. After cooling, 0.02 g of UV-sterilized ferrous ammonium sulfate was added, and the medium was stored under UV sterilization prior to use.

High-pressure immersion tests were conducted using coupon specimens (50 mm × 10 mm × 3 mm), with three specimens prepared for each condition. Prior to testing, the coupons were ground sequentially with 200#, 400#, and 800# abrasive papers, cleaned with deionized water and alcohol, dried, and weighed.

The experiments were performed in an F3-30/350 static high-pressure autoclave at 40 °C for 14 days. The total pressure was 10 MPa, with CO_2 partial pressures of 0.25 MPa and 0.5 MPa and chloride ion concentrations of 15,000 mg/L and 50,000 mg/L. Before testing, the autoclave was purged with N_2 for 2 h to remove oxygen, followed by the sequential introduction of CO_2 and N_2 to reach the target pressure.

3. Results and discussion

3.1. Analysis of corrosion rate

To evaluate the corrosion resistance of the three steels under combined high Cl^- concentration and CO_2 conditions, their average corrosion rates and maximum pitting depths were compared, as summarized in **Table 1**. The results show that uniform corrosion and pitting corrosion exhibit different trends under varying environmental conditions.

Under the condition of Cl^- 50,000 mg/L and P_{CO_2} 0.5 MPa, all three steels exhibited their highest average corrosion rates. Among them, the quenched and tempered antibacterial steel showed the lowest corrosion rate, while the conventional steel and the hot-rolled antibacterial steel exhibited higher values. When P_{CO_2}

was reduced to 0.25 MPa, the average corrosion rates of all steels decreased by approximately one order of magnitude, and the differences among the three materials were reduced. Under the condition of Cl^-: 15,000 mg/L and PCO_2: 0.5 MPa, the corrosion rates of all steels were lower than those under higher Cl^- concentration, and the difference among the three materials further decreased.

Regarding pitting corrosion, under the condition of Cl^- 50,000 mg/L and PCO_2 0.5 MPa, the maximum pitting depths of the two antibacterial steels were lower than that of the conventional steel. When CO_2 decreased to 0.25 MPa, the maximum pitting depth of the conventional steel decreased significantly, whereas that of the two antibacterial steels showed only minor changes. Under the condition of Cl^- 15,000 mg/L and P CO_2 0.5 MPa, the conventional steel exhibited the lowest maximum pitting depth among the three materials.

Table 1. Corrosion rates and maximum pitting depths of test specimens under high-pressure conditions

Material	Average Corrosion Rate, mm/a			Maximum Pitting Depth, um		
	$[Cl^-]$ 50000mg/L	$[Cl^-]$ 50000mg/L	$[Cl^-]$ 15000mg/L	$[Cl^-]$ 50000mg/L	$[Cl^-]$ 50000mg/L	$[Cl^-]$ 15000mg/L
	P_{CO_2} 0.5MPa	P_{CO_2} 0.25MPa	P_{CO_2} 0.5MPa	P_{CO_2} 0.5MPa	P_{CO_2} 0.25MPa	P_{CO_2} 0.5MPa
Hot-rolled Antibacterial Steel	0.1673	0.0119	0.0341	9.5120	9.8080	6.4300
Quenched and Tempered Antibacterial Steel	0.1162	0.0164	0.0262	11.3610	12.0720	4.1630
Conventional Steel	0.1405	0.0129	0.0363	23.6840	11.0550	2.5530

3.2. Micromorphology and elemental analysis of corrosion products

Under PCO_2 0.5 MPa and Cl^- 50,000 mg/L, the hot-rolled antibacterial steel showed a relatively continuous biofilm with locally agglomerated corrosion products, while the quenched and tempered antibacterial steel exhibited a loose, cracked film with sparsely distributed corrosion products (**Figure 1**). The conventional steel surface showed dispersed bacterial colonies without continuous film coverage. Under PCO_2 0.25 MPa and Cl^- 50,000 mg/L, both antibacterial steels formed thick biofilm layers with abundant corrosion products and surface cracks, whereas the conventional steel exhibited fewer corrosion products, mainly in localized aggregates. Under PCO_2 0.5 MPa and Cl^- 15,000 mg/L, the hot-rolled antibacterial steel showed abundant but scattered corrosion products, the quenched and tempered antibacterial steel exhibited only localized spherical products, and the conventional steel formed a dense,

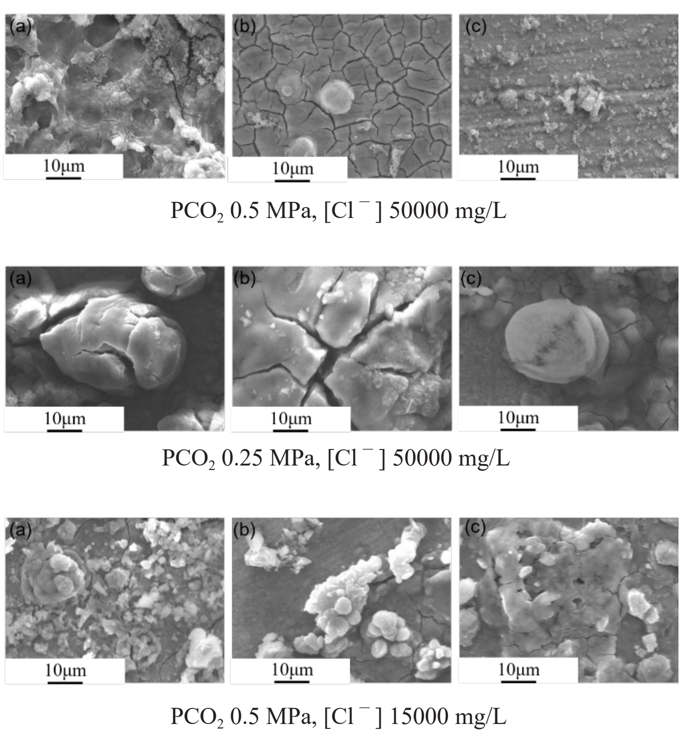

Figure 1. SEM of corrosion products on hot-rolled antibacterial, quenched and tempered antibacterial, and conventional steels. (a) Hot-rolled; (b) Quenched and tempered; (c) Conventional

widely distributed corrosion product layer.

3.3. Microscopic corrosion morphology

The substrate morphologies after removal of corrosion products are shown in **Figure 2**, revealing localized corrosion features of the three steels under different conditions.

Under PCO_2 0.5 MPa and Cl^- 50,000 mg/L, the conventional steel exhibited the most severe localized corrosion, with interconnected pits and the deepest pit morphology. The hot-rolled antibacterial steel showed relatively uniform dissolution, while the quenched and tempered antibacterial steel exhibited the least corrosion. Under PCO_2 0.25 MPa and Cl^- 50,000 mg/L, the hot-rolled antibacterial steel showed more pronounced localized surface deterioration, whereas the quenched and tempered antibacterial steel exhibited a lighter corrosion morphology. Despite a slightly higher average corrosion rate, the quenched and tempered steel showed more uniform surface dissolution, while corrosion on the hot-rolled antibacterial steel was concentrated in limited areas. Under PCO_2 0.5 MPa and Cl^- 15,000 mg/L, the hot-rolled antibacterial steel exhibited fewer pits, while the conventional and quenched and tempered steels showed a higher number of pits. The hot-rolled antibacterial steel tended to form fewer but deeper pits, whereas the other two steels exhibited more numerous but shallower pits.

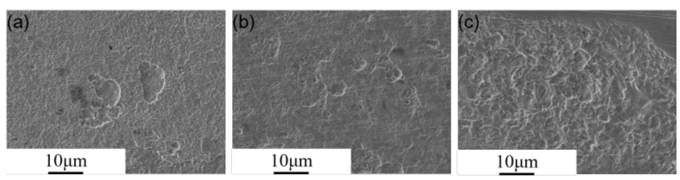

PCO_2 0.5 MPa, $[Cl^-]$ 50000 mg/L

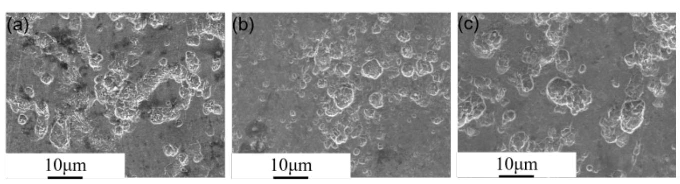

PCO_2 0.25 MPa, $[Cl^-]$ 50000 mg/L

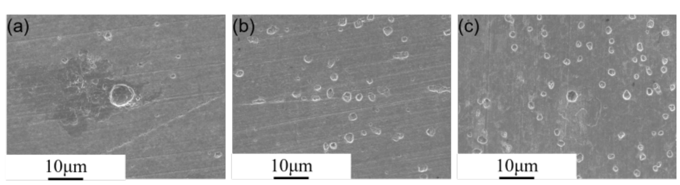

PCO_2 0.5 MPa, $[Cl^-]$ 15000 mg/L

Figure 2. Surface morphologies after removal of corrosion products on hot-rolled antibacterial, quenched and tempered antibacterial, and conventional steels (a) Hot-rolled; (b) Quenched and tempered; (c) Conventional

4. Conclusions

A combined analysis of corrosion rates, pitting depths, corrosion products, and substrate morphologies shows that high CO_2 partial pressure together with high Cl^- concentration leads to the most severe corrosion in all three steels. Under these conditions, both uniform corrosion and localized pitting were intensified. The quenched and tempered antibacterial steel consistently exhibited the lowest average corrosion rate, while the hot-rolled antibacterial steel showed the highest. In terms of pitting, both antibacterial steels exhibited shallower pits than the conventional steel, which developed the deepest localized corrosion.

Micromorphological observations indicate distinct corrosion features among the materials. The hot-rolled antibacterial steel formed dense biofilm–corrosion product layers, the quenched and tempered antibacterial steel showed loose and cracked films with dispersed corrosion products, and the conventional steel exhibited corrosion initiated at discrete surface sites. The conventional steel showed a transition between deep localized corrosion and widespread shallow corrosion depending on environmental conditions.

Overall, the results indicate that corrosion behavior in high Cl^- and high CO_2 environments is strongly related to material microstructure, biofilm characteristics, and corrosion product morphology.

Disclosure statement

The authors declare no conflict of interest.

References

[1] Zhang RJ, Cao ZZ, Zhang GX, et al., 2021, Research Progress of SRB Effect on Corrosion of Oil and Gas Pipelines. Corrosion Protection, 42(10): 68–73 + 108.

[2] Bhat S, Kumar B, Prasad S, et al., 2011, Failure Analysis: Failure of a New 8-in Pipeline from Group Gathering Station to Central Tank Farm. Materials Performance, 50(5): 50–54.

[3] Zhang H, Liu D, Zhao L, et al., 2022, Review on Corrosion and Corrosion Scale Formation Upon Unlined Cast Iron Pipes in Drinking Water Distribution Systems. Journal of Environmental Sciences, 2022(117): 173–189.

[4] Sharma M, Liu H, Tsesmetzis N, et al., 2022, Diagnosing Microbiologically Influenced Corrosion at a Crude Oil Pipeline Facility Leak Site—A Multiple Lines of Evidence Approach. International Biodeterioration & Biodegradation, 2022(172): 105438.

[5] Pei WX, 2024, Research on SRB Corrosion Behavior of X65 Pipeline Steel, thesis, Xian Shiyou University.

[6] Shi XB, Yang CG, Yan W, et al., 2019, Microbiologically Influenced Corrosion of Pipeline Steels. Journal of Chinese Society for Corrosion and Protection, 39(1): 9–17.

[7] King RA, Miller JDA, Smith JS, 1973, Corrosion of Mild Steel by Iron Sulphides. British Corrosion Journal, 8(3): 137–141.

[8] Tang HY, Holmes DE, Ueki T, et al., 2019, Iron Corrosion via Direct Metal-Microbe Electron Transfer. mBio, 10(3): e00303-19. https://doi.org/10.1128/mBio.00303-19

[9] Yang K, Shi XB, Yan W, et al., 2020, Novel Cu-Bearing Pipeline Steels: A New Strategy to Improve Resistance to Microbiologically Influenced Corrosion for Pipeline Steels. Acta Metallurgica Sinica, 56(4): 385–399.

[10] Song YF, 20205, Effects of FB/SRB/TGB on Viscosity of Polymer Solution and Treatment Methods, thesis, Northeast Petroleum University.

[11] Shi X, Zeng Y, Ren Y, et al., 2024, Effect of Nano-sized Cu-Rich Phase on Microbiological Corrosion Behavior of Cu and Ni-Added Steel for Oil Country Tubular Goods. ISIJ International, 64(6): 1047–1056.